



# Adsorption of perchlorate from aqueous solution by the calcination product of Mg/(Al–Fe) hydrotalcite-like compounds

Yiqiong Yang, Naiyun Gao\*, Wenhai Chu, Yongji Zhang, Yan Ma

State Key Laboratory of Pollution Control and Resources Reuse, Tongji University, Shanghai 200092, China

## ARTICLE INFO

### Article history:

Received 23 November 2011

Received in revised form 9 January 2012

Accepted 9 January 2012

Available online 16 January 2012

### Keywords:

Mg/(Al–Fe) hydrotalcite compounds

Calcination

Perchlorate

Adsorption

## ABSTRACT

The calcination products containing Mg(II), Al(III), and Fe(III) in the brucite-like layers with varying Mg/Al/Fe molar ratios at 550 °C were used as the adsorbent to remove perchlorate from aqueous solution, while the Mg/(Al–Fe) hydrotalcite compounds were synthesized by co-precipitation method at a constant pH value. The Mg/(Al–Fe) hydrotalcite compounds (HMAF) were characterized by XRD, FT-IR and TG–DTA. The characteristics showed that the layered double hydroxides structures in the HMAF were lost during calcination at 550 °C, but were reconstructed subsequent to adsorption of perchlorate, indicating that the ‘memory effect’ appeared to play an important role in perchlorate adsorption. Batch adsorption studies were conducted under various equilibration conditions, such as molar ratios of Mg/Al/Fe, calcined temperature, different initial solution pH, adsorbent dose, initial perchlorate concentration, and co-existing anions. It was found that the existence of ferric iron in calcined Mg/(Al–Fe) hydrotalcite compound (CHMAF) was favorable to removal of perchlorate from water, and the best ratio of Mg/Al/Fe is 3:0.8:0.2 (CHMAF5%). This study demonstrated that the calcination product of Mg/(Al–Fe) hydrotalcite-like compound was a promising adsorbent for control of the perchlorate pollution in water.

© 2012 Elsevier B.V. All rights reserved.

## 1. Introduction

Perchlorate is widely known to be an inorganic endocrine disruptor because it is a potent competitive inhibitor of sodium-iodide symporter (NIS) on the basolateral membrane of thyroid cells [1]. Perchlorate ( $\text{ClO}_4^-$ ), used as an oxidizer and explosive in the areas such as rocket propellants [2], fireworks manufacturing, arm industry, automobile airbags and any other civilian applications, is attracting increasing attention as an inorganic contaminant in drinking water, ground water, and surface water. Numbers recent studies have reported that perchlorate has been detected in drinking water, groundwater, and surface water in many countries, such as USA [3,4], Japan [5], Korea [6,7], India [8], Deutschland [9] and China [10]. Because of its high mobility, extremely low concentrations in water, and strong resistance to traditional water treatment technologies, perchlorate has become one of the greatest challenges of the water industry. Besides water, perchlorate has been recently found in soil, vegetation, food and saliva, especially leafy

vegetables and bovine milk [11–13], indicating that the emerging pollutant has entered the human and environmental food chains. These reports have raised substantial concern among the public and water regulatory agencies, as a response, several states in the United States have established their own action levels of perchlorate in water.

Current technologies available for remediation of perchlorate-contaminated water, such as surfactant modified-activated carbon, biological treatment and ion exchange systems are some of the technologies that are being used [14]. Among these treatment methods, adsorption process is very attractive due to low cost and high treatment efficiency. In our previous work, the removal of perchlorate onto iron modified activated carbon was examined, and the results showed that iron modified activated carbon could removal perchlorate effectively from water [15].

Just recently, a class of anionic clays known as layered double hydroxides (LDHs) of hydrotalcite-like compounds (HTlc) has been paid substantial attention to with the general chemical formula:  $[\text{M}_{1-x}\text{M}_x^{3+}(\text{OH})_2]^{x+}(\text{A}_{x/n}^{n-})\cdot m\text{H}_2\text{O}$  [16], where  $\text{M}^{2+}$  and  $\text{M}^{3+}$  are divalent and trivalent metal ions, and  $x$  is the ratio  $\text{M}^{3+}/(\text{M}^{2+} + \text{M}^{3+})$ .  $\text{M}^{2+}$  and  $\text{M}^{3+}$  ions with ionic radii close to that of  $\text{Mg}^{2+}$  are accommodated in the brucite-like layers consisting of edge-sharing octahedral units which are stacked one on top of the other. HTlc can uptake anions from water via three mechanisms: (i) adsorption on the external surface; (ii) intercalation by anion exchange;

\* Corresponding author at: State Key Laboratory of Pollution Control and Resources Reuse, Ministry of Education, College of Environmental Science and Engineering, Tongji University, Shanghai 200092, China. Tel.: +86 21 65982691; fax: +86 21 65986313.

E-mail address: [gaonaiyun1@126.com](mailto:gaonaiyun1@126.com) (N.Y. Gao).

and (iii) intercalation by reconstruction of calcined products. The last one is also known as “structure memory effect” [17,18], in which hydrotalcite-like compounds are calcined to eliminate most of the interlayer anions, and then anions can be incorporated during rehydration to “recover” the calcined HTlc to their original layered structures. The formed mixed oxides are mostly amorphous, with a high specific surface area and an ability to recover the layered structure in contact with water [19]. A large number of HTlc has been studied in water treatments in the last decades, the most studied are the aluminum based ones such as Mg/Al hydrotalcites and their calcined products [20–22]. However, two drawbacks have limited application of such materials in drinking water treatment: first, Al can potentially develop or accelerate the Alzheimer syndrome in human beings [23]; and second, there is a technical difficult to separate the adsorbents from water. Considering these scenarios, the critical step to successfully use HTlc for removal of perchlorate from water is to develop a new, cost-effective, toxic-free, and readily separated layered double hydroxides material. There fore, in order to reduce Al content, as well as try not to affect the adsorption capacity as much as possible, Al was substituted partly for ferric iron in our study. So Mg/(Al–Fe) hydrotalcite compounds were synthesized and modified by calcination.

The objective of this study is to synthesize new Mg/(Al–Fe) hydrotalcite compounds (HMAF), and evaluate its technical feasibility to adsorb perchlorate from water. Bench scale studies were conducted to first assess the effects of the factors relevant to calcination of the adsorbent on perchlorate removal, including calcination temperature and the molar ratio of Mg, Al and Fe, and then characterize the adsorbent material via XRD, FT-IR, and thermogravimetric analysis. Thereafter, the kinetics and isotherm patterns of adsorption of perchlorate on the calcined Mg/(Al–Fe) hydrotalcite compounds (CHMAF) were determined. Finally, the effects of the factors associated with solution chemistry, such as initial solution pH, adsorbent dose, initial perchlorate concentration, and competitive anions, were determined.

## 2. Materials and methods

### 2.1. Materials

All the solutions were prepared with bidistilled (conductivity level  $\leq 1 \mu\text{s}/\text{cm}$ ).  $\text{Mg}(\text{NO}_3)_2 \cdot 6\text{H}_2\text{O}$ ,  $\text{Al}(\text{NO}_3)_3 \cdot 9\text{H}_2\text{O}$ ,  $\text{Fe}(\text{NO}_3)_3 \cdot 9\text{H}_2\text{O}$ , NaOH,  $\text{Na}_2\text{CO}_3$  and  $\text{NaClO}_4$  were A.R. grade and used as received. The perchlorate ( $\text{ClO}_4^-$ ) aqueous solution was prepared to dissolve certain amount of  $\text{NaClO}_4$  to water. An appropriate volume of 0.1 mol/L  $\text{HNO}_3$  or NaOH solutions was used to adjust the pH of the solution.

### 2.2. Synthesis of adsorbents

Low supersaturation coprecipitation with constant pH was used for the synthesis of HTlc materials.

The layered double hydroxides MgAlFe HTlc (HMAF<sub>x</sub>; here,  $x$  is the mol.% of Fe) with different  $\text{Mg}^{\text{II}}:\text{Al}^{\text{III}}:\text{Fe}^{\text{III}}$  molar ratios (3:1:0, 3:0.8:0.2, 3:0.6:0.4 and 3:0.2:0.8) were prepared by low supersaturation co-precipitation method at constant pH. The mixed solution containing metal nitrates of  $\text{Mg}^{\text{II}}$ ,  $\text{Al}^{\text{III}}$  and  $\text{Fe}^{\text{III}}$  with desired concentrations ( $[\text{Mg}] + [\text{Al}] + [\text{Fe}] = 1 \text{ mol}$ ), 2 mol NaOH and 0.5 mol  $\text{Na}_2\text{CO}_3$  were added simultaneously to a 1 L beaker at the rate of 50 mL/h under constant vigorous stirring condition at 75 °C at the pH of 7–8. The precipitate formed was aged for 24 h at 75 °C at the end of which the precipitate was separated by filter. This was followed by repeated washing with deionized water until the effluent solution was neutral. The wet solid was slowly dried at 85 °C for 24 h to obtain the HMAF. The HMAF was calcined at 550 °C for 4 h to obtain

the calcined hydrotalcites signed as CHMAF<sub>x</sub> (here,  $x$  is the mol.% of Fe).

### 2.3. Adsorbents characterization

Powder X-ray diffraction (XRD) analysis was performed using a D8 Advance XRD diffractometer with Cu-K $\alpha$  radiation ( $\lambda = 1.54184 \text{ \AA}$ , 40 kV and 40 mA) at a scanning rate of 10°/min. Scanning diffraction angle range is set as 5–90°. The adsorbent materials were pelletized with KBr for the FTIR study. FTIR spectra were recorded in the range 4000–400/cm<sup>-1</sup> with a Nicolet 5700 spectrometer. TG–DTA measurements were carried out using a Pyris Diamond TG/DTA instrument (Q600 SDT) with N<sub>2</sub> as carrier gas. The temperature was controlled within a range of 50–800 °C and at a rate of 10 °C/min.

### 2.4. Adsorption experiments

A stock solution containing 10 mg/L perchlorate was prepared by  $\text{NaClO}_4$ . Batch experimental solutions were diluted for adsorption and analysis. The experiments were carried out in 200 mL stoppered conical flasks under constant shaking (200 rpm) in a thermostat shaker. Adsorption isotherms were conducted with initial perchlorate concentrations of 200, 400, 1000, 2000, 4000 and 5000  $\mu\text{g}/\text{L}$  at 25 °C and the contact time of 24 h. Solution pH was not controlled during the reaction. After 24 h, the mixing was stopped, and the mixed solution was filtered by 0.45  $\mu\text{m}$  membrane. The residual perchlorate in the filtrate was quantified using an ion chromatograph (Dionex, ICs2000) equipped with a suppressed conductivity detector, an AS20 column, an AG20 guard column, and a 250  $\mu\text{L}$  sample loop (detection limit = 4  $\mu\text{g}/\text{L}$ ). A degassed 35 mmol/L sodium hydroxide solution was used as eluent.

The effect of contact time was carried out at specific time intervals of 30, 60, 100, 150, 200, 300, 400, 500, 600, 700, 800, 1440 and 2880 min with the initial perchlorate concentration of 2000  $\mu\text{g}/\text{L}$  at 25 °C. The pH effect was studied within the range of 2.0–12.0 (adjusted with 0.1 mol/L  $\text{HNO}_3$  or NaOH) with the initial perchlorate concentration of 2000  $\mu\text{g}/\text{L}$  and the contact time of 24 h at 25 °C.

Above batch experiments were conducted under the same conditions of 150 mL perchlorate solution and adsorbent dose of 1.3 g/L. All experiments were carried out in duplicates and the deviation about the mean was less than five percent in all cases.

### 2.5. Calculations

At each designated sampling time, 5 mL sample was collected for perchlorate analysis. Perchlorate removal by the CLDH at a specific time  $t$  was defined as follows (Eq (1)):

$$q_t = \frac{(C_0 - C_t)V}{m} \quad (1)$$

where  $q_t$  is the amount of adsorbed perchlorate at time  $t$  ( $\mu\text{g}/\text{g}$ );  $V$  is the solution volume (liters);  $C_0$  and  $C_t$  are the initial and remaining perchlorate concentrations in solution before reaction and at time  $t$  ( $\mu\text{g}/\text{L}$ ), respectively; and  $m$  is the mass of the adsorbent (g).

Linear (Eq. (2)) [24], Freundlich (Eq. (3)) [25] and Tempkin (Eq. (4)) [26] isotherms were assessed to fit the experimental data, as shown in Eqs. (2), (3), and (4), respectively.

$$q_e = K_r C_e + b \quad (2)$$

$$q_e = K_F C_e^n \quad (3)$$

$$q_e = B \ln A + B \ln C_e \quad (4)$$

where  $q_e$  is the amount of adsorbed perchlorate per mass unit CHMAF at equilibrium ( $\mu\text{g}/\text{g}$ );  $q_{\text{max}}$  is the saturated monolayer

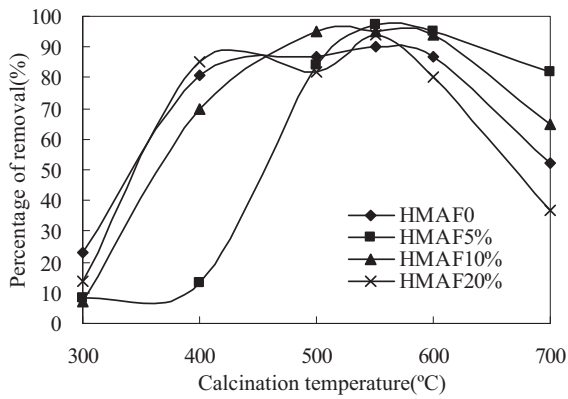


Fig. 1. Effect of calcination temperature on the  $\text{ClO}_4^-$  removal efficiency (the initial  $\text{ClO}_4^-$  concentration was  $2000 \mu\text{g/L}$ ,  $\text{CHMAF} = 1.33 \text{ g/L}$ ,  $25^\circ\text{C}$ ).

adsorption capacity ( $\mu\text{g/g}$ );  $K_r$  is the binding energy of the adsorption system ( $\text{L}/\mu\text{g}$ ), and,  $b$  is the Linear constant;  $C_e$  is the equilibrium concentration in bulk solution ( $\mu\text{g/L}$ );  $K_F$  is the Freundlich constant;  $n$  is the adsorption intensity; and,  $B$  and  $A$  are the Temkin constants.

Four kinetic models were examined to fit the experimental data.

The pseudo-first order model, i.e. the Lagergren model, is the most commonly used adsorption kinetics model, as follows [27]:

$$\ln(q_e - q_t) = \ln q_e - k_1 t \quad (5)$$

where  $k_1$  is the rate constant of adsorption ( $\text{min}^{-1}$ );  $q_e$  and  $q_t$  are the adsorption loadings of perchlorate on the adsorbent ( $\mu\text{g/g}$ ) at equilibrium and at time  $t$  (min), respectively; and  $t$  is the reaction time.

The pseudo-second order equation is established on the assumption that the occupation rate of adsorption sites is proportional to the square of the number of unoccupied sites (Eq. (6)) [28]:

$$\frac{t}{q_t} = \frac{1}{k_2 q_e^2} + \frac{t}{q_e} \quad (6)$$

where  $k_2$  ( $\text{g}/\mu\text{g min}$ ) is the rate constant of pseudo-second-order adsorption.

The Elovich equation is given as follows (Eq. (7)) [29]:

$$q_t = \beta \ln(\alpha\beta) + \beta \ln t \quad (7)$$

where  $\alpha$  and  $\beta$  are the initial adsorption rate ( $\mu\text{g/g min}$ ) and the desorption constant ( $\text{g}/\mu\text{g}$ ).

The diffusion rate of the perchlorate ion in a particle,  $k_i$ , can be calculated from the following linear equation (Eq. (8)) [30]:

$$q_t = k_i t^{0.5} \quad (8)$$

where  $k_i$  is the intraparticle diffusion rate ( $\mu\text{g/g min}^{0.5}$ ).

### 3. Results and discussion

The adsorption of perchlorate from aqueous solution by the calcination product of  $\text{Mg}/(\text{Al}-\text{Fe})$  hydrotalcite-like compound was studied from the following aspects: structure characteristics, removal mechanism and the adsorption properties.

#### 3.1. Structure characteristics

##### 3.1.1. Calcination temperature

The effect of calcination temperature on adsorption of perchlorate is shown in Fig. 1. For any molar percent of ferric (0–20%), the perchlorate adsorption exhibited a similar pattern at different calcination temperatures. The removal efficiency

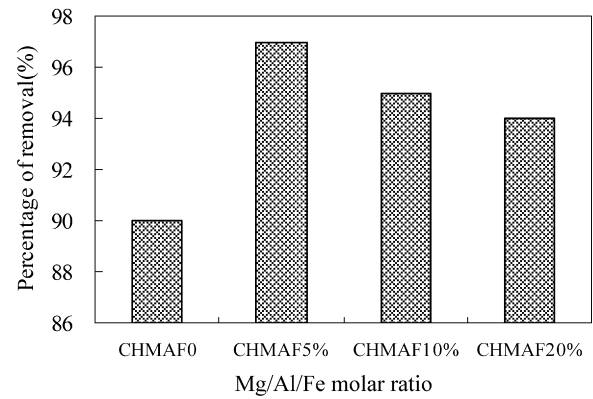


Fig. 2. Effect of  $[\text{Mg}]/[\text{Al}]/[\text{Fe}]$  on the  $\text{ClO}_4^-$  removal efficiency (the initial  $\text{ClO}_4^-$  concentration was  $2000 \mu\text{g/L}$ ,  $\text{CHMAF} = 1.33 \text{ g/L}$ , adsorbents calcined at  $550^\circ\text{C}$ ,  $25^\circ\text{C}$ ).

was increased with the increasing temperature from 300 to  $550^\circ\text{C}$ , but significantly dropped when the calcination temperature declined from 600 to  $700^\circ\text{C}$ . Perchlorate adsorption capacity of the  $\text{Mg}/(\text{Al}-\text{Fe})$  hydrotalcite-like compounds were closely related to their structural properties formed during calcination. Reconstruction occurred only at a specific calcination temperature range that was adequately high to achieve thermal decomposition and thus eliminate most of the carbonate in the interlayer. However, a too high calcination temperature could lead to the formation of stable spinel and  $\text{MgO}$  phases, so that hydrotalcites could not be reconstructed [31]. In this study, the most favorable calcination temperature range was observed at  $550^\circ\text{C}$ .

##### 3.1.2. Molar ratio of $[\text{Mg}]/[\text{Al}]/[\text{Fe}]$

The effect of  $[\text{Mg}]/[\text{Al}]/[\text{Fe}]$  on the perchlorate adsorption is shown in Fig. 2. The perchlorate removal peaked at CHMAF5% ( $[\text{Mg}^{2+}]/[\text{Al}^{3+}]/[\text{Fe}^{3+}] = 3:0.8:0.2$ , 97%), followed by CHMAF10% ( $[\text{Mg}^{2+}]/[\text{Al}^{3+}]/[\text{Fe}^{3+}] = 3:0.6:0.4$ , 95%), then the CHMAF20% ( $[\text{Mg}^{2+}]/[\text{Al}^{3+}]/[\text{Fe}^{3+}] = 3:0.2:0.8$ ) and CHMAF0 ( $[\text{Mg}^{2+}]/[\text{Al}^{3+}]/[\text{Fe}^{3+}] = 3:1:0$ ), the removal rates were 94% and 90%, respectively. Generally, during the CHMAF reconstruction, calcinated hydrotalcite-like compounds adsorption of perchlorate could be enhanced by the existence of  $\text{Fe}^{3+}$  to the brucite-like sheet. Triantafyllidis et al. [32] indicated that the replacement of  $\text{Al}^{3+}$  by  $\text{Fe}^{3+}$  in layered double hydroxide strengthens the bond between double-hydroxide layers and carbonates in the interlayer by increasing the positive surface charge. However, the crystal structure of HMAF might be destroyed when too much  $\text{Fe}^{3+}$  entered the brucite-like sheet. Therefore, an optimal  $[\text{Mg}^{2+}]/[\text{Al}^{3+}]/[\text{Fe}^{3+}]$  typically existed to achieve the highest charge density in the HMAF layers and maximize the net adsorption. In summary, the best adsorption samples was prepared at an calcination temperature of  $550^\circ\text{C}$  and  $[\text{Mg}^{2+}]/[\text{Al}^{3+}]/[\text{Fe}^{3+}] = 3:0.8:0.2$ .

#### 3.2. Removal mechanism

The extent of crystalline of the samples and their calcination products were determined by XRD analysis. Fig. 3 shows the diffraction patterns of the HMAF (HMAF0, HMAF5%, HMAF10%, HMAF20%), CHMAF (CHMAF0, CHMAF5%, CHMAF10%, CHMAF20%) and CHMAF $\text{ClO}_4$  (CHMAF0, CHMAF5%, CHMAF10% and CHMAF20% after adsorption). It is shown that all the diffraction pattern of the HMAF have sharp and symmetric peaks at lower  $2\theta$  (003, 006 and 009), which are characteristics as the hydrotalcite-like compounds and a high degree of crystallinity [33]. More over, it shows that the characteristic peaks of HMAF0 decrease a little from the lower intensities and the smaller interlayer space by replacing with increased content of  $\text{Fe}^{3+}$ . As we know that the interlayer space

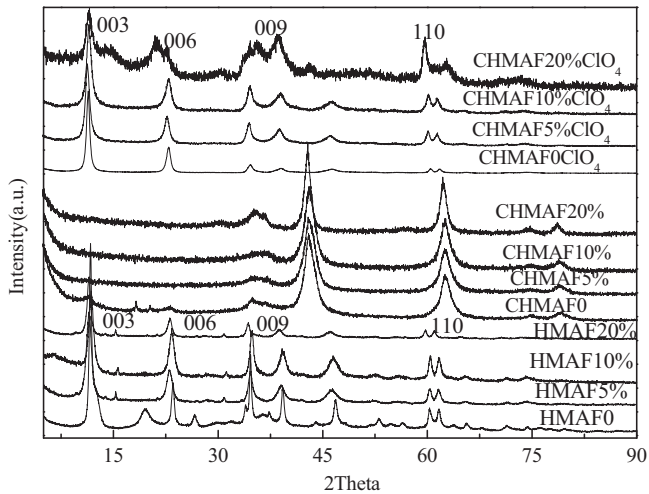


**Fig. 3.** Powder XRD patterns for HMAF0, HMAF5%, HMAF10%, HMAF20%, CHMAF0, CHMAF5%, CHMAF10%, CHMAF20%, and CHMAF after uptake of perchlorate ion.

depends on  $M^{2+}/M^{3+}$  molar ratio, metal ionic radius, the size of anion within the interlayer and the degree of hydration [34]. Therefore, the minor difference of d-spacing may be due to the larger ionic radius of ferric iron than aluminum ion [35].

While the layered hydrotalcite-like structure is lost after calcination at  $550^\circ\text{C}$  with characteristic peaks (003) and (006) of hydrotalcite disappeared. That means that the hydrotalcite structure is seriously destroyed and there is disordering in the stacking of the layers.

Upon adsorption of perchlorate, CHMAF again exhibited these unique characteristics as a result of reconstruction. The result indicates that the Mg/(Al-Fe) hydrotalcite-like compound has the “memory effect” structure.

The FT-IR spectra of the HMAF, CHMAF, and CHMAF after perchlorate adsorption are shown in Fig. 4. In the FT-IR spectra of HMAF, the band observed at  $3432$ ,  $3458$ ,  $3455$  and  $3450\text{ cm}^{-1}$  respectively with the increase of content of  $\text{Fe}^{3+}$  were due to the vibration of structural OH groups hydrogen bonded with interlamellar water molecules or OH groups in brucite-like layers [36]. A large width of the band indicated that hydrogen bonds existed within a broad range of strength. The band at  $1384\text{ cm}^{-1}$  corresponded to the V3 (an asymmetric stretching mode) of the

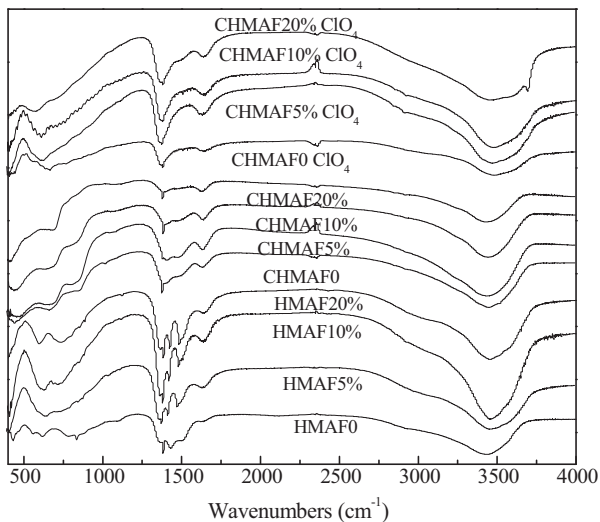


**Fig. 4.** FT-IR spectra for HMAF0, HMAF5%, HMAF10%, HMAF20%, CHMAF0, CHMAF5%, CHMAF10%, CHMAF20%, and CHMAF after uptake of perchlorate ion.

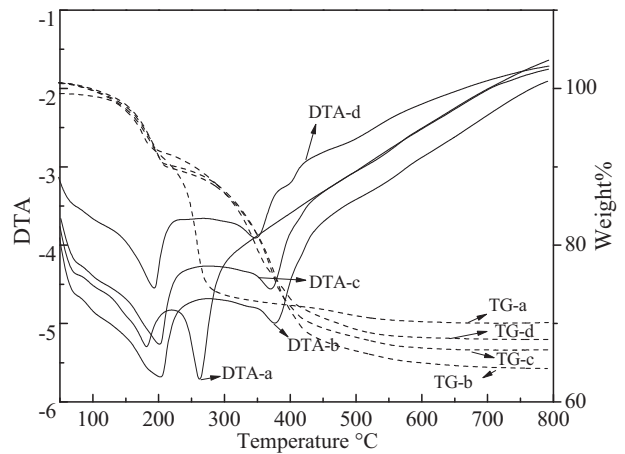


**Fig. 5.** TG-DTA profiles for (a) HMAF0, (b) HMAF5%, (c) HMAF10% and (d) HMAF20%.

carbonate anions. The peaks at  $1431\text{ cm}^{-1}$  (HMAF0),  $1637\text{ cm}^{-1}$  (HMAF5%, HMAF10%, HMAF20%)  $\text{cm}^{-1}$  might be caused by the bending mode of water molecules and interlamellar carbonate ions (carbonate ions are most likely present during hydrolysis of the metal salts), it seems like that the band shifted to much higher due to the ferric replace aluminum partly. The band  $1384\text{ cm}^{-1}$  disappeared after calcination of  $550^\circ\text{C}$  and reappeared during the adsorption of perchlorate. This could indicate that the surface adsorption of carbonate anions is a property of CHMAF [37]. This observation was in good agreement with our XRD data.

The thermal behaviors of the HMAF and CHMAF after uptake of perchlorate were analyzed through TG-DTA experiments. As seen in Figs. 5 and 6, both HMAF and CHMAF after uptake of perchlorate exhibited weight loss at three temperature ranges. The first drop with the increasing temperature from  $50$  to  $220^\circ\text{C}$ , due to the removal of surface adsorbed and interlayer water molecules. The endothermic peak between  $250^\circ\text{C}$  and  $400^\circ\text{C}$  is mainly caused by the evaporation of crystal water in HMAF and CHMAF after uptake of perchlorate. Endothermic peaks at  $430$  and  $600^\circ\text{C}$  with a significant weight loss can be ascribed to the decomposition of interlayer anion and the formed  $\text{H}_2\text{O}$  and  $\text{CO}_2$  escaped. TG-DTA results of HMAF and CHMAF after uptake of perchlorate are shown in Table 1.

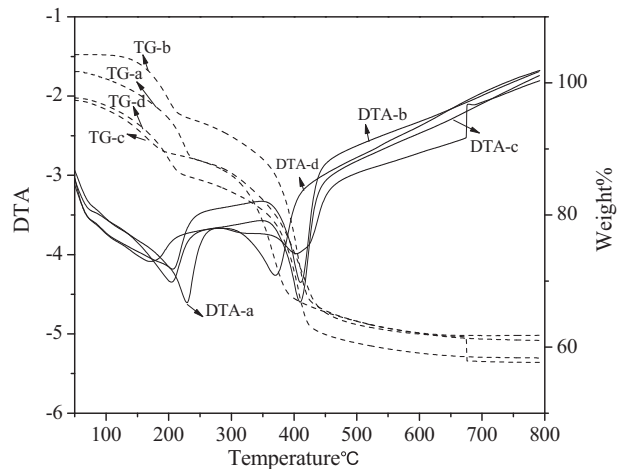


**Fig. 6.** TG-DTA profiles for (a) CHMAF0ClO<sub>4</sub>, (b) CHMAF5% ClO<sub>4</sub>, (c) CHMAF10% ClO<sub>4</sub> and (d) CHMAF20% ClO<sub>4</sub>.

**Table 1**  
TG–DTA results of HMAF and CHMAF after uptake perchlorate.

Sample	The first weight loss/%	The first endo tem/°C	The second weight loss/%	The second endo tem/°C	The third weight loss/%	The third endo tem/°C
HMAF0	6.21	178	19.39	257	29.68	479
HMAF5%	12.11	198	30.88	378	42.88	528
HMAF10%	11.95	195	29.93	369	41.15	528
HMAF20%	10.03	189	27.10	347	38.87	461
CHMAF0ClO <sub>4</sub>	9.23	223	29.11	414	42.02	675
CHMAF5%ClO <sub>4</sub>	11.85	202	30.98	407	37.20	429
CHMAF10%ClO <sub>4</sub>	10.64	200	30.29	406	36.31	431
CHMAF20%ClO <sub>4</sub>	7.00	188	20.67	368	27.89	430

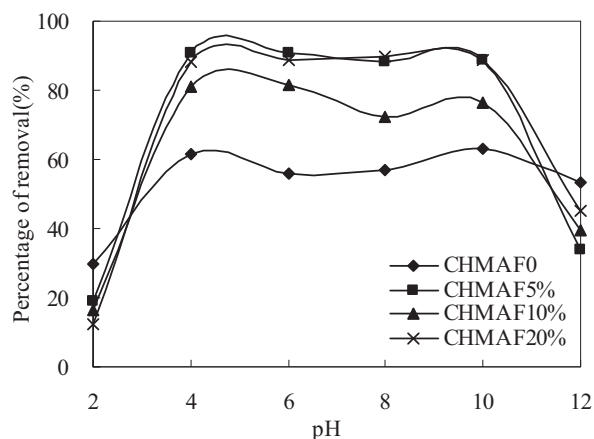


**Fig. 7.** Effect of pH on the removal of ClO<sub>4</sub><sup>-</sup> (the initial ClO<sub>4</sub><sup>-</sup> concentration was 2000 µg/L, CHMAF = 1.33 g/L, 25 °C).

### 3.3. Adsorption properties

#### 3.3.1. Effect of initial solution pH

The effect of initial solution pH (2.0–12.0) on CHMAF adsorption of perchlorate is shown in Fig. 7. The perchlorate removal efficiency was increased from 30% to 62%, 19% to 91%, 16% to 81% and 13% to 88% while the ferric molar percent increases from 0% to 20% respectively, when the initial solution pH went up from 2 to 4. At a too low pH (<4), the decrease in ClO<sub>4</sub><sup>-</sup> adsorption was probably caused by dissolution of the adsorbents. As shown in Fig. 9, a high concentration of Mg<sup>2+</sup> was released into solution at too low pH (<4), and the structure of CHMAF was possibly disordered. At pH 4–10, they almost plateaued. Of interest, at an initial solution pH of 4–10, CHMAF exhibited a strong buffering capacity, and the final solution pH was within a narrow range of 11.26–11.55 as shown in Fig. 8. As a result, dissolved Mg<sup>2+</sup>, Al<sup>3+</sup> in solution were <5 mg/L and <1.5 mg/L,

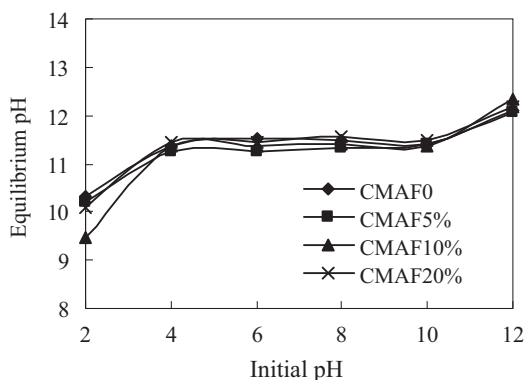


**Fig. 8.** Effect of CHMAF on the equilibrium pH (the initial ClO<sub>4</sub><sup>-</sup> concentration was 2000 µg/L, CHMAF = 1.33 g/L, 25 °C).

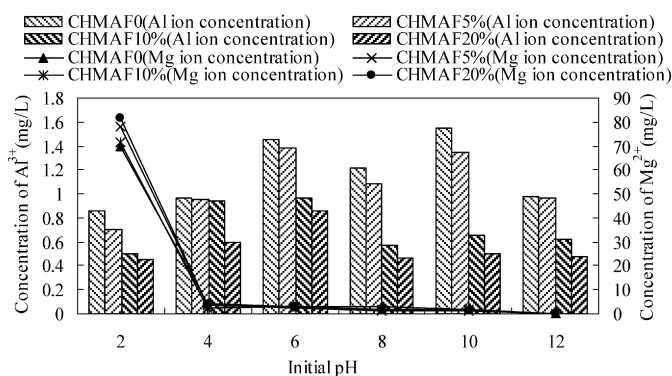


**Fig. 9.** Concentration of metal ions in resulting solution (the initial ClO<sub>4</sub><sup>-</sup> concentration was 2000 µg/L, CHMAF = 1.33 g/L, 25 °C).

respectively. However, once the initial pH dropped from 10 to 12, the removal rate significantly declined to 53.30%, 33.80%, 39.57% and 45.07% respectively, probably because a too high pH might enhance competition of hydroxides with perchlorate for active sites on the adsorbent. Figs. 7 and 9 revealed that the removal efficiency was improved, and the concentration of dissolved metal had been suppressed due to the addition of Fe<sup>3+</sup> in hydrotalcite-like compound. Bruna et al. [38] also stated that the presence of Fe<sup>3+</sup> in hydrotalcite would increase the attraction of anions in the inter-layer by layers due to the greater polarizing power of Fe<sup>3+</sup> than Al<sup>3+</sup> and makes its displacement more difficult.

#### 3.3.2. Effect of adsorbent dose

Effect of the adsorbent dose on perchlorate removal and adsorption capacity is shown in Fig. 10. Generally, a high CHMAF dose accomplished a high perchlorate removal because more adsorbents meant more available active sites to bind perchlorate from water. Of note, all of CHMAF exhibited a two-phase adsorption pattern

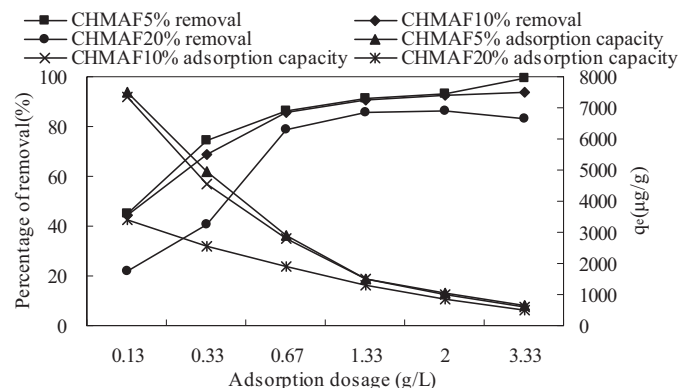


**Fig. 10.** Effect of dosage on ClO<sub>4</sub><sup>-</sup> removal by CHMAF (the initial ClO<sub>4</sub><sup>-</sup> concentration was 2000 µg/L, 25 °C).

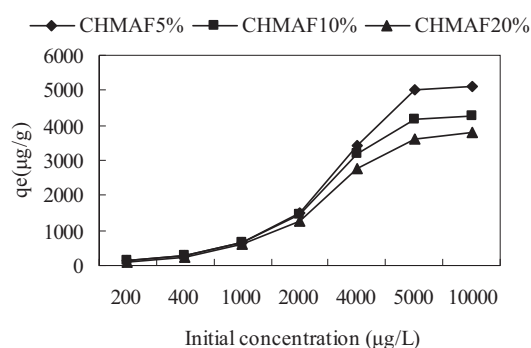


**Fig. 11.** Effect of initial concentration on the removal efficiency (CHMAF = 1.33 g/L, 25 °C).

in perchlorate adsorption with the increasing dose. As the CHMAF dose increased from 0.13 to 1.33 g/L, the removal efficiency was dramatically increased from 45% to 92% (CHMAF5%), 45% to 91% (CHMAF10%) and 22% to 86% (CHMAF20%). However, when the dose continued to increase to 3.33 g/L, the perchlorate removal slightly went up to 99%, 94% and 83% respectively. In contrast, the adsorption capacity had a different behavior with the increasing adsorbent dose. As the dose was increased from 0.13 to 3.33 g/L, the adsorption capacity almost linearly declined. In the subsequent tests, the adsorbent dose used was 1.33 g/L.

### 3.3.3. Effect of initial perchlorate concentration

Effect of the initial perchlorate concentration (200–10,000  $\mu\text{g/L}$ ) on the adsorption capacity is shown in Fig. 11. It can be seen that the adsorption capacity of perchlorate increases with the increase of the perchlorate concentration. The adsorption capacity was nearly linearly increased with the increasing initial perchlorate concentration. While the initial concentration reached to 5000  $\mu\text{g/L}$ , adsorption capacity did not change significantly and the  $q_e$  for CHMAF5%, CHMAF10% and CHMAF20% are 5001  $\mu\text{g/g}$ , 4167  $\mu\text{g/g}$  and 3605  $\mu\text{g/g}$  respectively.

Current technologies for adsorption of perchlorate-contaminated water mainly focus on granular activated carbon (GAC). The GAC-based iron compounds could remove 86% perchlorate (initial concentration is 4 mg/L) at dosage of 20 g/L in 12 h at 25 °C, with 0.172 mg/g adsorption capacity [15]. Na et al. [39] demonstrated that GAC preloaded with iron-oxalic acid has enhanced perchlorate adsorption with 0.34 mg/g adsorption capacity, and the tailored GAC could provide a service life of up to 70 days when compared to only 40 days with virgin GAC. Komarneni et al. [40] evaluated As-synthesized MCM-41 has a higher removal of perchlorate with  $0.378 \pm 0.038$  meq/g than the cationic surfactant modified activated carbon sample, which removed  $0.304 \pm 0.005$  meq/g.

In summary, virgin GAC or molecular sieve has limited capacity for perchlorate adsorption and requires tailoring to make it practically feasible, but this makes it more expensive and the adsorption also requires disposal of perchlorate laden spent carbon or regenerative brine. The results showed that the calcination product of Mg/(Al–Fe) hydrotalcite-like compounds had more strong perchlorate adsorption capacity than other adsorbents and it was a promising adsorbent for control of the perchlorate pollution in water.

### 3.3.4. Effect of co-existing anions on perchlorate adsorption by adsorbent

Effects of common water anions on the perchlorate adsorption capacity on CHMAF are shown in Fig. 12. The anions included sulfate, chloride, nitrate, dihydrogen phosphate and carbonate ions.

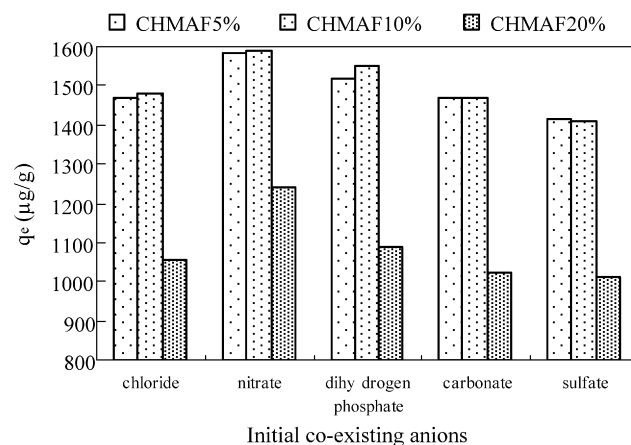


**Fig. 12.** Effects of co-existing anions on the removal efficiency (the initial  $\text{ClO}_4^-$  concentration was 2000  $\mu\text{g/L}$ , the concentration of  $\text{Cl}^-$ ,  $\text{NO}_3^-$ ,  $\text{H}_2\text{PO}_4^-$ ,  $\text{CO}_3^{2-}$  and  $\text{SO}_4^{2-}$  = 5 mg/L, CHMAF = 1.33 g/L, 25 °C).

Typically, all the anions showed an inhibiting effect on the CMF3 adsorption of perchlorate, and the inhibiting degree was increased with the increasing quantivalency. It can be seen from Fig. 12 that nitrate can hardly influence the adsorption capacity of perchlorate for CHMAF5% and CHMAF10%. Effect of co-existing anions on adsorption capacity of perchlorate increases with the following order:  $\text{NO}_3^- < \text{H}_2\text{PO}_4^- < \text{Cl}^- < \text{CO}_3^{2-} \approx \text{SO}_4^{2-}$ , i.e., multivalent anions are adsorbed more readily than monovalent anions. On the other hand, the influence of  $\text{CO}_3^{2-}$  in this system is especially significant because of the “memory effect”, for the  $\text{CO}_3^{2-}$  ions have the priority to be adsorbed onto CHMAF to resume its original structure. It is noteworthy that co-existing anions play a significant impact on the adsorption of perchlorate by CHMAF20%. That maybe the higher iron content, the smaller interlayer space is, so, perchlorate is difficult to enter the layer.

### 3.4. Kinetic studies

Measured data and modeled data in the kinetics tests for perchlorate adsorption are shown in Fig. 13 and Table 2. The order of the four kinetics models with regards toward the fitting of measured and modeled data was pseudo-second-order kinetics model > first-order kinetics model > Elovich equation model  $\gg$  inter-particle diffusion model in terms of coefficient of determination ( $R^2$ ). Among the first three acceptable kinetics models, pseudo-second-order kinetics model appeared to best describe perchlorate removal by CHMAF adsorption. Moreover, both CHMAF5% and CHMAF10% could reduce 85% perchlorate within 300 min.

### 3.5. Adsorption isotherm

Measured data and model data in the adsorption isotherm tests for perchlorate are shown in Fig. 14 and Table 3. For the initial perchlorate concentration is very low (2000  $\mu\text{g/L}$ ), here, the Linear, Freundlich and Tempkin isotherms were used to fit experimental data. As seen, the linear isotherm was the best one to describe the CHMAF adsorption of perchlorate at 25 °C with the highest  $R^2$  of 0.9992 (CHMAF10%), 0.9946 (CHMAF20%) and 0.9934 (CHMAF5%). The experimental data for isotherm modeling are the results determined from initial concentration effect. The adsorption intensity  $n$  in Freundlich isotherm for CHMAF5%, CHMAF10% and CHMAF20% are 1.1214, 1.3562 and 1.2712 respectively, all of them are close to 1, confirms that the Linear isotherms fit the measured data best as well.

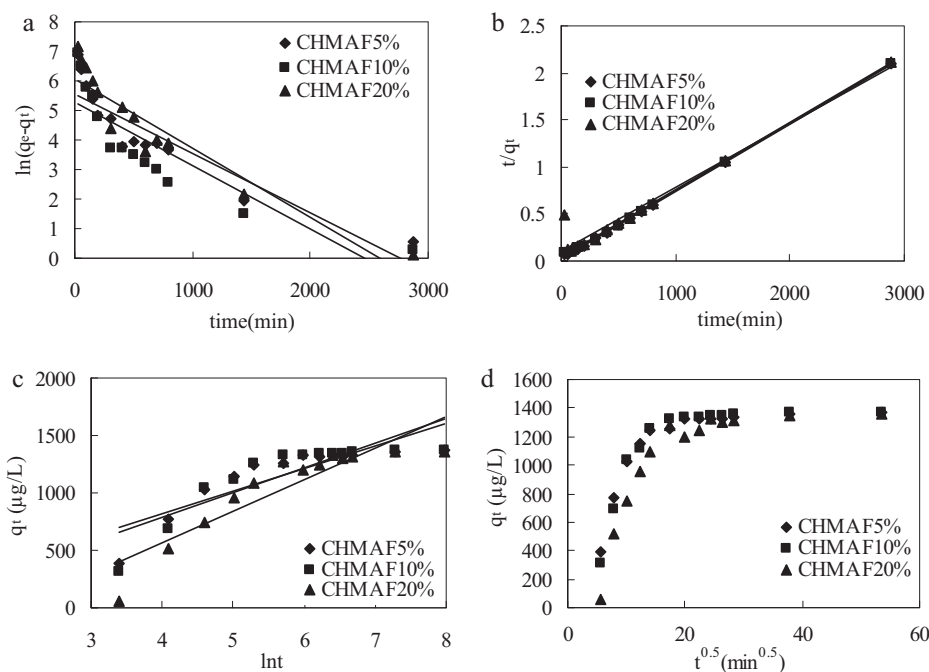


**Fig. 13.** (A) First-order kinetics model, (B) pseudo-second-order kinetics model, (C) Elovich equation model, (D) inter-particle diffusion model (initial  $\text{ClO}_4^-$  concentration was 2000  $\mu\text{g/L}$ , CHMAF = 1.33  $\text{g/L}$ , 25  $^\circ\text{C}$ ).

**Table 2**

Comparison between adsorption parameters of Lagergren pseudo-first, pseudo-second order, Elovich equation and inter-particle diffusion models.

CHMAF	Pseudo-first-order			Pseudo-second order			Elovich equation			Inter-particle	
	$k_1$	$q_e$	$R^2$	$k_2$	$q_{e,cal}$	$R^2$	$\alpha$	$\beta$	$R^2$	$k_i$	$R^2$
CHMAF5%	0.0029	257.5207	0.8300	$1.88 \times 10^{-5}$	1428.571	0.9996	0.0063	195.03	0.7512	43.865	-2.0387
CHMAF10%	0.0022	195.3905	0.7419	$1.90 \times 10^{-5}$	1428.571	0.9990	0.0034	214.27	0.7304	44.200	-1.4695
CHMAF20%	0.0024	438.3423	0.8765	$5.02 \times 10^{-6}$	1428.571	0.9556	0.0005	277.66	0.8150	41.795	-0.1434

**Table 3**

Calculated equilibrium constants.

CHMAF	Linear			Freundlich			Tempkin		
	$K_T$	$b$	$R^2$	$K_F$	$n$	$R^2$	$A$	$B$	$R^2$
CHMAF5%	9.8922	-205.33	0.9934	4.2453	1.1214	0.9779	0.030773	1433.7	0.8360
CHMAF10%	8.1933	-263.95	0.9992	0.9056	1.3562	0.9793	0.017454	1608.2	0.9174
CHMAF20%	2.8949	-57.43	0.9946	0.4764	1.2712	0.9372	0.009213	1306.0	0.9536

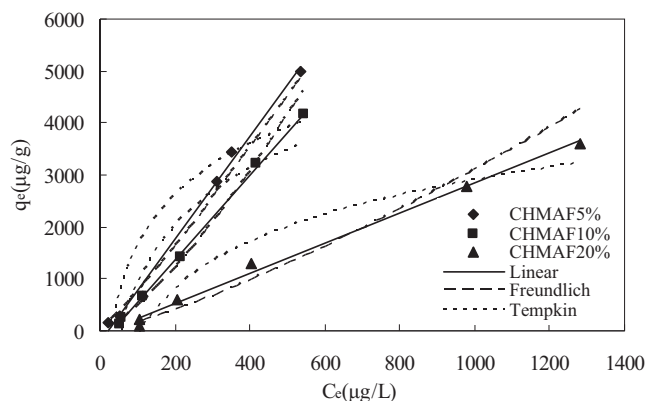


**Fig. 14.** Isotherm adsorption of perchlorate by CHMAF at 25  $^\circ\text{C}$ .

## 4. Conclusions

In this study, the calcination product of  $\text{Mg}/(\text{Al}-\text{Fe})$  hydrotalcite-like compounds were synthesized, which can be an efficient adsorbent for perchlorate from water. XRD analysis showed that the layered hydrotalcite-like structure of the HMAF was lost during calcination at 550  $^\circ\text{C}$ , but was reconstructed after the adsorption of perchlorate. The so-called “memory effect” appeared to play a significantly important role in perchlorate adsorption. The calcination temperature of 550  $^\circ\text{C}$  and a molar ratio of  $\text{Mg}/\text{Al}/\text{Fe}$  at 3:0.8:0.2 (CHMAF5%) were the optimal conditions for the adsorbent synthesis. Both CHMAF5% and CHMAF10% could reduce 85% perchlorate within 300 min at a broad initial pH range of 4.0–10.0 when initial perchlorate concentration is 2000  $\mu\text{g/L}$ . Such an adsorption kinetics pattern could be well described by a pseudo-second-order reaction model. On the other hand, Linear adsorption isotherm models better explained the perchlorate adsorption data at 25  $^\circ\text{C}$ . Furthermore, the solution chemistry factors including solution pH, dose

of the adsorbent, initial perchlorate concentration, and competitive anions could affect the efficiencies of perchlorate adsorption to the different CHMAF. Moreover, the presence of  $\text{Fe}^{3+}$  in hydrotalcite would increase the attraction of perchlorate in the interlayer by layers and suppress the concentration of dissolved metal. The study here in demonstrates the calcination product of  $\text{Mg}/(\text{Al}-\text{Fe})$  hydrotalcite-like compound is a promising alternative adsorbent for perchlorate-contaminated water.

### Acknowledgments

This work was supported by the National Natural Science Foundation of China (No. 50878163 and No. 51178321), the National Major Project of Science & Technology Ministry of China (No. 2008ZX07421-002), and the Research and Development Project of Ministry of Housing and Urban-Rural Development (No. 2009-K7-4).

### References

- [1] A.M. Leung, E.N. Pearce, L.E. Braverman, Perchlorate, iodine and the thyroid, *Best Pract. Res. Clin. Endocrinol. Metab.* 24 (2010) 133–141.
- [2] E.T. Urbansky, Perchlorate chemistry: implications for analysis and remediation, *Biochem. J.* 2 (1998) 81–95.
- [3] K.H. Kucharzyk, R.L. Crawford, B. Cosens, T.F. Hess, Development of drinking water standards for perchlorate in the United States, *J. Environ. Manage.* 91 (2009) 303–310.
- [4] D.R. Parker, A.L. Seyfferth, B.K. Reese, Perchlorate in groundwater: a synoptic survey of “pristine” sites in the coterminous United States, *Environ. Sci. Technol.* 42 (2008) 1465–1471.
- [5] K. Kosaka, M. Asami, Y. Matsuoka, M. Kamoshita, S. Kunikane, Occurrence of perchlorate in drinking water sources of metropolitan area in Japan, *Water Res.* 41 (2007) 3474–3482.
- [6] O. Quiñones, J.E. Oh, B. Vanderford, J.H. Kim, J. Cho, S.A. Snyder, Perchlorate assessment of the Nakdong and Yeongsan watersheds, Republic of Korea, *Environ. Toxicol. Chem.* 26 (2007) 1349–1354.
- [7] H. Namguk, J. Hyunchan, K. Jeong, Occurrence of perchlorate in Drinking Water and Seawater in South Korea, *Arch. Environ. Contam. Toxicol.* 61 (2011) 166–172.
- [8] K. Kannan, M.L. Praamsma, J.F. Oldi, T. Kunisue, R.K. Sinha, Occurrence of perchlorate in drinking water, groundwater, surface water and human saliva from India, *Chemosphere* 76 (2009) 22–26.
- [9] J.S. Traugott, F. Jessika, J.P. Carol, Untersuchung ausgewählter Oberflächen-, Grund- und Bodenwasserproben auf Perchlorat in Deutschland: Erste Ergebnisse, *Grundwasser-Zeitschrift der Fachsektion Hydrogeologie* 16 (2011) 37–43.
- [10] Q. Wu, T. Zhang, H.W. Sun, Perchlorate in tap water, groundwater, surface waters, and bottled water from China and its association with other inorganic anions and with disinfection byproducts, *Arch. Environ. Contam. Toxicol.* 58 (2010) 543–550.
- [11] A.B. Kirk, E.E. Smith, K. Tian, T.A. Anderson, P.K. Dasgupta, Perchlorate in milk, *Environ. Sci. Technol.* 37 (2003) 4979–4981.
- [12] A.B. Kirk, P.K. Martinelango, K. Tian, A. Dutta, E.E. Smith, P.K. Dasgupta, Perchlorate and iodide in dairy and breast milk, *Environ. Sci. Technol.* 39 (2005) 2011–2017.
- [13] C.A. Sanchez, B.C. Blount, L. Valentin-Blasini, S.M. Lesch, R.I. Krieger, Perchlorate in the feed-dairy continuum of the southwestern United States, *J. Agric. Food Chem.* 56 (2008) 5443–5450.
- [14] S. Rangesh, A.S. George, Treatment of perchlorate in drinking water: a critical review, *Sep. Purif. Technol.* 69 (2009) 7–21.
- [15] J.H. Xu, N.Y. Gao, Y.L. Tang, Y. Deng, M.H. Sui, Perchlorate removal using granular activated carbon supported iron compounds: synthesis, characterization and reactivity, *J. Environ. Sci.* 22 (2010) 1807–1813.
- [16] K.H. Goh, T.T. Lim, Z.L. Dong, Application of layered double hydroxides for removal of oxyanions: a review, *Water Res.* 42 (2008) 1343–1368.
- [17] M. Dinesh, U.P. Charles, Arsenic removal from water/wastewater using adsorbents—a critical review, *J. Hazard. Mater.* 142 (2007) 1–53.
- [18] J. Cornejo, R. Celis, I. Pavlovic, M.A. Ulibarri, Interactions of pesticides with clays and layered double hydroxides: a review, *Clay Miner.* 43 (2008) 155–176.
- [19] L. Yang, Z. Shahrivari, P.K.T. Liu, Removal of trace levels of arsenic and selenium from aqueous solutions by calcined and uncalcined layered double hydroxides (LDH), *Ind. Eng. Chem. Res.* 44 (2005) 6804–6815.
- [20] W. Ma, N.N. Zhao, G. Yang, L.Y. Tian, R. Wang, Removal of fluoride ions from aqueous solution by the calcination product of  $\text{Mg}-\text{Al}-\text{Fe}$  hydrotalcite-like compound, *Desalination* 268 (2011) 20–26.
- [21] J.Y. Kim, S. Komarneni, R. Parette, F. Cannon, H. Katsuki, Perchlorate uptake by synthetic layered double hydroxides and organo-clay minerals, *Appl. Clay Sci.* 51 (2011) 158–164.
- [22] L. Lv, J. He, M. Wei, D.G. Evans, X. Duan, Uptake of chloride ion from aqueous solution by calcined layered double hydroxides: equilibrium and kinetic studies, *Water Res.* 40 (2006) 735–743.
- [23] J. Das, B.S. Patra, N. Baliarsingh, K.M. Parida, Calcined  $\text{Mg}-\text{Fe}-\text{CO}_3$  LDH as an adsorbent for the removal of selenite, *J. Colloid Interface Sci.* 316 (2007) 216–223.
- [24] A. Agrawal, K.K. Sahu, B.D. Pandey, A comparative adsorption study of copper on various industrial solid wastes, *AIChE J.* 50 (2004) 2430–2438.
- [25] S. Pradhan, S.S. Shukla, K.L. Dorris, Removal of nickel from aqueous solutions using crab shells, *J. Hazard. Mater. B* 125 (2005) 201–204.
- [26] S. Deng, Y.P. Ting, Fungal biomass with grafted poly (acrylic acid) for enhancement of  $\text{Cu}(\text{II})$  and  $\text{Cd}(\text{II})$  biosorption, *Langmuir* 21 (2005) 5940–5948.
- [27] N.K. Lazaridis, D.D. Asouhidou, Kinetics of sorptive removal of chromium (VI) from aqueous solutions by calcined  $\text{Mg}-\text{Al}-\text{CO}_3$  hydrotalcite, *Water Res.* 37 (2003) 2875–2882.
- [28] Y.S. Ho, G. McKay, Sorption of dye from aqueous solution by peat, *Chem. Eng. J.* 70 (1998) 115–124.
- [29] G. McKay, Y.S. Ho, J.C.Y. Ng, Biosorption of copper from waste waters: a review, *Sep. Purif. Meth.* 28 (1999) 87–125.
- [30] M. Jansson-Charrier, E. Guibal, J. Roussy, Vanadium sorption by chitosan: kinetic and equilibrium, *Water Res.* 30 (1996) 465–475.
- [31] M. Shigeo, Physico-chemical properties of synthetic hydrotalcites in relation to composition, *Clay. Clay Miner.* 28 (1980) 50–56.
- [32] K.S. Triantafyllidis, E.N. Peleka, V.G. Komvokis, P.P. Mavros, Iron-modified hydrotalcite-like materials as highly efficient phosphate sorbents, *J. Colloid Interface Sci.* 342 (2010) 427–436.
- [33] F. Cavani, F. Trifiro, A. Vaccari, Hydrotalcite-type anionic clays: preparation, properties and applications, *Catal. Today* 11 (1991) 173–301.
- [34] O.P. Ferreira, S.G. de Moraes, N. Duran, L. Cornejo, O.L. Alves, Evaluation of boron removal from water by hydrotalcites-like compounds, *Chemosphere* 62 (2006) 80–88.
- [35] L.L. Xiao, W. Ma, M. Han, Z.H. Cheng, The influence of ferric iron in calcined nano- $\text{Mg}/\text{Al}$  hydrotalcite on adsorption of  $\text{Cr}(\text{VI})$  from aqueous solution, *J. Hazard. Mater.* 186 (2011) 690–698.
- [36] M.A. Ulibarri, I. Pavlovic, C. Barriga, M.C. Hermosín, Adsorption of anionic species on hydrotalcite-like compounds: effect of interlayer anion and crystallinity, *Appl. Clay Sci.* 18 (2001) 17–27.
- [37] J.I.D. Cosimo, V.K. Diez, M. Xu, E. Iglesia, C.R. Apesteguia, Structure and surface and catalytic properties of  $\text{Mg}-\text{Al}$  basic oxides, *J. Catal.* 178 (1998) 499–510.
- [38] F. Bruna, R. Celis, I. Pavlovic, C. Barriga, J. Cornejo, M.A. Ulibarri, Layered double hydroxides as adsorbents and carriers of the herbicide (4-chloro-2-methylphenoxy) acetic acid (MCPA): systems  $\text{Mg}-\text{Al}$ ,  $\text{Mg}-\text{Al}-\text{Fe}$ , *J. Hazard. Mater.* 168 (2009) 1476–1481.
- [39] C. Na, F.S. Cannon, B. Hagerup, Perchlorate removal via iron-preloaded GAC and borohydride regeneration, *J. AWWA* 94 (2002) 90–102.
- [40] S. Komarneni, J.Y. Kim, R. Parette, F.S. Cannon, As-synthesized MCM-41 silica: new adsorbent for perchlorate, *J. Porous Mater.* 17 (2010) 651–656.